THE JOURNAL OF PHYSICAL CHEMISTRY C

pubs.acs.org/JPCC Article

Mixed-Valence Magnetic Molecular Cell for Quantum Cellular Automata: Prospects of Designing Multifunctional Devices through Exploration of Double Exchange

Andrew Palii,* Juan Modesto Clemente-Juan,* Sergey Aldoshin, Denis Korchagin, Andrey Rybakov, Shmuel Zilberg, and Boris Tsukerblat*

Cite This: J. Phys. Chem. C 2020, 124, 25602−25614

ABSTRACT: In this article, we propose to use multielectron square-planar mixed-valence (MV) molecules as molecular cells for quantum cellular automata (QCA) devices. As distinguished from previous proposals in this area, in multielectron cells, the electronic pair encoding binary information is shared among localized spins ("spin cores"). Hopefully, this will allow exploring not only charge degrees of freedom encoding binary information in the antipodal electronic distributions but also spin degrees of freedom through the magnetic interactions such as double exchange and Heisenberg−Dirac−Van Vleck (HDVV) exchange. To develop the proposed route, the square-planar tetrameric cells for QCA have been theoretically modeled. The considered cells comprise a pair of excess electrons shared among four spin cores and hence they exhibit double exchange and HDVV exchange. Such cells can be based either on the square-planar mixed-valence molecular clusters or on the similar square arrays of multielectron quantum dots. The detailed case study of the cell representing the transition-metal tetramer of the type of $d^2-d^2-d^1-d^1$ shows that depending on the relative strength of the second-order double exchange and HDVV exchange, the isolated cell has either ground localized spin-triplet or one of the two delocalized spin-singlets, exhibiting different extents of electron delocalization. Due to different sensitivities of these states to the quadrupole electrostatic field induced by the polarized neighboring driver cell, the latter is shown to be able to produce switching between different ground states (including spin-switching between spin-singlet and spin-triplet), which leads to the nonmonotonic behavior of the cell−cell response function. This opens new perspectives for the designing of multifunctional devices combining the QCA functionality with spin-switching function.

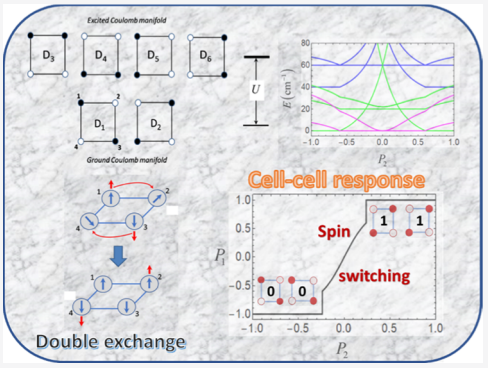

1. INTRODUCTION

Topicality of the study of QCA is determined by the importance of the technology based on QCA, which has potential in competing with the traditional metal-oxide-semiconductor (CMOS) technology for manufacturing of logic elements for digital integrated circuits. Studies of the last decade[1−4] inspire hope in the prospects of the novel QCA principles of nanotechnology and practical feasibility of the design of electronic devices. Being currentless in their nature, QCA circuits ensure ultralow heat release as compared with CMOS. Due to this advantage, QCA devices are of great potential importance to perform computations at very high switching rates.

The paradigm of QCA is free of the main difficulty peculiar to the concept of quantum computing in which the binary information is stored in the eigenvectors of a two-level quantum system (qubits) and therefore its practical application is strongly limited by the requirement of coherence. In contrast, the problem of coherence does not constrain applicability of systems proposed for use in computing with QCA because the binary information in such systems is stored in charge distributions (rather than in qubits) in the QCA cells and is transmitted between the cells via the classical Coulomb forces.

The initial proposal of the QCA device has been based on the quantum dot cells coupled via the Coulomb interaction to form a cellular automata architecture.[1,5−12] Each such cell typically consists of four quantum dots situated in the vertices of a square and two extra electrons tunneling between these dots. Further development led to the idea of molecular QCA, which can be regarded as a next step in miniaturization of QCA based on quantum dots.[13−16] Additional expected

Received: September 8, 2020
Revised: October 27, 2020
Published: November 6, 2020

https://dx.doi.org/10.1021/acs.jpcc.0c08186
J. Phys. Chem. C 2020, 124, 25602−25614

substantial advantages of molecular systems as candidates to be implemented as QCA cells are the following: (1) unlike quantum dots, the molecular system of a specified chemical composition is absolutely identical and therefore has identical physical characteristics; (2) by a proper chemical synthesis, the molecular clusters can be engineered to have the desired physical characteristics that can be controlled by the due choice of the metal ions, ligands, etc.; (3) the electronic subsystem of a molecule is usually coupled to molecular vibrations but well isolated from the thermal bath (phonons in solids), which ensures very small heat release in course of the QCA action; and (4) finally, molecules can be attached to different types of platforms by grafting individual clusters or monolayers on solid surfaces; due to the molecular size of the cells, one can reach extremely high density of devices, which does not produce critical heat release.

Mixed-valence complexes containing mobile excess electrons can be viewed as natural candidates to act as molecular cells, which would satisfy the above requirements. The role of quantum dots in such molecules is played by the redox sites, which are linked by the bridging ligands mediating the electron tunneling. The problem of the rational design of MV molecular cells is of crucial importance for the area of molecular QCA.[16−28] The key requirement to the "working cells" is that they must be bistable to be able to encode binary information in two quasistable charge configurations. The two states of the cell arise from two charge distributions, which encode binary **0** and **1**. These states are degenerate in an isolated cell, but the degeneracy is removed and one of these configurations becomes the ground state if the cell interacts with the polarized neighboring "driver cell". Altering the driver-cell-induced electrostatic perturbation forces the working cell to switch between the two states. The second requirement is that the switching between the two configurations of the functioning cell should occur in a nonlinear abrupt manner. This means that the molecule acting as a molecular cell should have high polarizability with respect to the external electrostatic perturbation switching cell between configurations **0** and **1**. The search for MV complexes satisfying these requirements represents a rather difficult task, and thus the number of reported such kinds of systems remains relatively scarce.

In the molecules proposed to date as cells, as well as in quantum dot cells, the excess electrons or holes are delocalized over the network of diamagnetic sites. Meanwhile, a special area of mixed valency dealing with the systems in which the extra particle jumps over paramagnetic sites (see, for example, reviews[29−32] and refs therein), which conventionally are referred to as "spin cores", remained unexplored in the molecular QCA projects. This area originated from solid-state physics[33−35] in which the concept of double exchange has been introduced and invoked to interpret ferromagnetism of perovskite crystals caused by spin-polarization of the ions by mobile electrons. Then, this concept of "spin-dependent delocalization" moved to chemistry and was explored in the study of complex ferredoxins.[33−36]

Such magnetic MV clusters are of current interest in molecular electronics and spintronics.[37−43] Also, one can expect that similar "physical molecules" exhibiting double exchange can be composed of magnetic quantum dots[44−46] comprising different numbers of unpaired electrons. In this regard, it is worthwhile revealing the possibility of using clusters comprising paramagnetic cores as tetrameric square-planar cells and thus considerably extending the class of systems suitable as QCA cells. Recently, a similar idea to explore a bidimeric system was proposed in ref 47. Hopefully, the use of the magnetic cells can expand their functionality due to additional advantages provided by spin degrees of freedom along with the charge degrees of freedom directly engaged in the encoding of binary information.

In the present study, we have attempted to shed light on this issue through the detailed theoretical modeling of the isolated and interacting square-planar cells based on MV transition-metal tetramer of the $d^2-d^2-d^1-d^1$ type in which both double exchange and HDVV exchange are operative. Along with the analysis of the functional characteristics of QCA based on multielectron cells, we discuss a possibility of obtaining an additional spin-switching function in the same device.

2. METHODS AND THEORY

2.1. Model Hamiltonian for a Free Tetrameric Square-Planar Cell: Double Exchange. In this section, we consider a free square-planar cell composed of four paramagnetic centers such as multielectron quantum dots or four redox sites in an MV molecule. For the sake of definiteness, we will use the terminology adopted in the area of mixed-valence molecules although the general results are applicable to both kinds of objects. It is supposed that the two extra electrons in the tetranuclear MV cluster are shared among four magnetic high-spin ions, which can be referred to as spin cores, and the electrons are ferromagnetically coupled to the core's spins according to Hund's rule. Usually, in the theory of mixed valency, the spin cores are represented by the localized electrons forming high-spin crystal field configurations, while the extra electrons move over empty orbitals.

In terms of the valence bond theory, there are six possible distributions of two extra electrons over four sites as shown in Figure 1. In two of these distributions (electronic configurations), the extra electrons are localized on the sites disposed along the diagonals, while in the remaining four configurations, the electrons occupy the positions situated along edges of the cell. The two diagonal electronic configurations (D_1 and D_2 in Figure 1) correspond to the minimum of the Coulomb repulsion and thus form the ground Coulomb manifold, while the remaining four configurations belong to the excited manifold separated from the ground manifold by the Coulomb energy gap U.

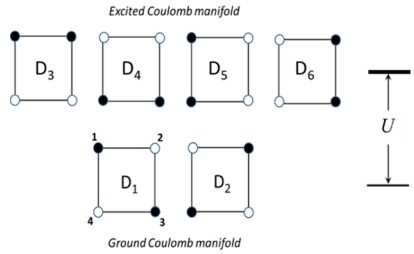

Figure 1. Scheme of the square-planar tetrameric cell and numeration of the sites, and different electronic distributions corresponding to the ground and excited Coulomb manifolds separated by the Coulomb energy gap U. The sites occupied by the extra electrons are shown by black balls, and the spin cores are indicated by white balls.

The subsequent consideration will be based on the model that involves three main ingredients: (1) Coulomb repulsion between instantly occupied sites; (2) electron transfer from occupied sites to spin cores; and (3) the HDVV exchange

https://dx.doi.org/10.1021/acs.jpcc.0c08186
J. Phys. Chem. C 2020, 124, 25602−25614

interaction between all kinds of pairs (d^2−d^2, d^1−d^1, d^2−d^1) of the magnetic sites in the square-planar structure. In many cases (at least in transition-metal complexes), the Coulomb repulsion acts as a leading contribution, and the electron transfer plays a role of physically significant interaction giving rise to the spin-dependent delocalization over the magnetic cores. As distinguished from previous considerations of a bielectronic square, in the system under consideration, the extra electrons jump over spin sites, which just constitutes the basis for considering the double exchange. As far as we are dealing with the magnetic ions, HDVV exchange should be taken into account along with the double exchange. As will be clarified later, the HDVV exchange, which normally is smaller than the double exchange, can play an important role due to the effect of the Coulomb reduction of the double exchange in the actual cases.

We thus arrive at the following t−J-Hamiltonian for a free tetrameric cell:

$$\hat{H}_{\text{free cell}} = \hat{H}_0 + \hat{V} \tag{1}$$

In eq 1, the term $\hat{H}_0$, defined as

$$\hat{H}_0 = \sum_{i<j} U_{i,j}\hat{n}_i\hat{n}_j \tag{2}$$

is the Hamiltonian of the Coulomb repulsion between the two extra electrons and $\hat{n}_i$ is the extra electron occupation operator for the site ($n_i = 1$ if site i contains an extra electron; otherwise, $n_i = 0$). Then, the term $\hat{V}$ is defined as

$$\hat{V} = \hat{H}_{\text{DE}} + \hat{H}_{\text{HDVV}} \tag{3}$$

This term includes the one-electron transfer $\hat{H}_{\text{DE}}$ (interrelated with the double exchange) and HDVV exchange ($\hat{H}_{\text{HDVV}}$).

In the presence of spin cores, the double exchange can be expressed through the electron-transfer Hamiltonian:

$$\hat{H}_{\text{DE}} = t \sum_{i<j,\sigma} (1 - \delta_{j,i+2})(c^+_{i,\sigma}c_{j,\sigma} + c^+_{j,\sigma}c_{i,\sigma}) \tag{4}$$

in which extra electrons are assumed to jump only between the nearest neighboring sites situated on the sides of the square (which is ensured by the presence of the Kronecker δ-symbol $\delta_{j,i+2}$), t is the corresponding transfer parameter, $c^+_{i,\sigma}$ and $c_{j,\sigma}$ are the standard creation and annihilation operators that act in the space of the orbitals available for the extra electron, and σ is the spin projection. It is to be noted that in the Hubbard-like Hamiltonian employed here the double occupancy of the orbitals available for the mobile electrons is explicitly excluded. Note also that the electron-transfer term $\hat{H}_{\text{DE}}$ mixes the states belonging to different distributions of the two extra electrons over four sites, which are different in the position of only one extra electron.

Finally, in the t−J model so far adopted, the orbital degrees of freedom are excluded, which means that the model is dealing with the system of orbitally nondegenerate magnetic cores and orbitals available for extra electrons. Alternatively, it is assumed that the ground crystal field terms of constituent d^n and d^{n+1} ions are orbital singlets well separated from the excited levels. We will resort to this traditional approximation in the double-exchange theory with two arguments in mind. (1) Usually, the magnetic ions in molecular polynuclear compounds reside in low site-symmetry positions so that the orbital degeneracy is completely removed. In particular, this means that the spin−orbit coupling is reduced to the second-order contribution giving rise to a relatively weak single-ion magnetic anisotropy. Under this condition, the zero-field splitting is rather small as compared to the remaining gaps in the energy pattern that will be drawn hereunder. (2) In those rare cases when the degeneracy is not completely lifted in the local crystal fields, the theoretical consideration of the double exchange not only becomes rather complicated but also loses its generality due to the presence of a large number of adjustable parameters (see ref 48) and additional conditions. That is why the present consideration is framed by a simplified model that provides the basic understanding of the properties of mixed-valence magnetic molecular cells.

2.2. Heisenberg−Van Vleck−Dirac Exchange in a Mixed-Valence Tetrameric Cell. Since the HDVV exchange acts within the system of localized spins, it requires a special notation as applied to an MV system with variable populations of magnetic sites. Assuming that the HDVV exchange is also restricted to pairs of nearest neighboring sites, one can express the HDVV Hamiltonian for an MV unit as

$$\hat{H}_{\text{HDVV}} = -2 \sum_{k\neq l} \hat{O}_{kl} \sum_{i<j} J^{(kl)}_{ij}(1-\delta_{j,i+2})\hat{S}_i\hat{S}_j \tag{5}$$

As distinguished from the electron-transfer term $\hat{H}_{\text{DE}}$, the term $\hat{H}_{HDVV}$ acts within the groups of spin states belonging to a certain distribution D_λ (λ = 1, 2, ..., 6, Figure 1). To explicitly take this into account, we have introduced the operators $\hat{O}_{kl}$ in which the indexes k and l indicate the sites of localization of the extra electron (i.e., a given electronic distribution). Being applied to the spin state of the tetramer belonging to the definite kl distribution, it gives the same state, whereas the application of this operator to the state arising from other distributions gives zero. Each distribution generates a specific set of exchange parameters, and so the exchange integrals in eq 5 are dependent on k and l. Thus, for k = 1 and l = 2, we have $J_{12} \equiv J_{n+1,n+1}$, $J_{14} = J_{23} \equiv J_{n+1,n}$, and $J_{34} \equiv J_{n,n}$, where $J_{n,n}$ is the exchange parameter describing the coupling between the two spin cores, each composed of n unpaired electrons, $J_{n+1,n}$ describes the coupling between the spin-core and the site containing n + 1 unpaired electrons (including one extra electron in addition to the core electrons), and finally $J_{n+1,n+1}$ relates to the interaction between the two centers, each occupied by an extra electron.

3. DISCUSSION

3.1. Combined Effect of the Double Exchange and Coulomb Repulsion. Here we focus on the illustrative case of the tetrameric cell in which the paramagnetic spin-core contains the only unpaired electron (d^1-type core) so that S_0 = 1/2. These systems can be referred to as d^2−d^2−d^1−d^1-type clusters that have six unpaired electrons. Although these systems are relatively simple, their study reveals common features of the phenomena we intend to discuss. When the extra electron is trapped (d^2 ion), its spin is coupled ferromagnetically to the core spin S_0 to give spin S_0 + 1/2 = 1, while the total spin of such a tetramer takes values S = 0, 1, 2, 3.

To elucidate the manifestation of the double exchange, in Figure 2a we present the low-lying part of the energy spectrum of the tetramer calculated considering the double-exchange interaction and the Coulomb repulsion (temporarily omitting the exchange interaction). The calculation of the energy spectrum presented in Figure 2a was performed with the aid of

https://dx.doi.org/10.1021/acs.jpcc.0c08186
J. Phys. Chem. C 2020, 124, 25602−25614

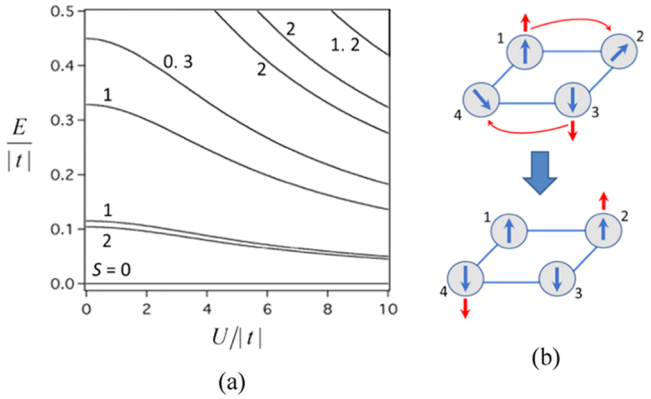

Figure 2. Combined effect of the double exchange and Coulomb interaction on the energy spectrum of the square-planar d^2−d^2−d^1−d^1 tetramer (a), and illustration of the antiferromagnetic spin-polarization effect in the tetrameric systems with two mobile electrons (b). All parameters of HDVV exchange are assumed to be vanishing. Only the low-lying part of the energy spectrum with labeling of the energy levels by the total spin values S is shown. The energy of the ground state is regarded as the reference energy.

the angular momentum approach and the MVPACK program based on this approach.[49−51]

It is remarkable that the ground state of the tetramer is diamagnetic ($S = 0$) independent of the interrelation between the double exchange and the Coulomb repulsion. This result appears to be in conflict with the basic paradigm according to which the double exchange gives rise to a ferromagnetic spin alignment in a pair of magnetic ions.[34] In fact, it is well-known that due to the ferromagnetic intra-atomic exchange coupling of the mobile spin with the localized ones (spin cores), the latter are polarized by the spin of excess electrons, which tends to align them in a parallel fashion.[31,52,53] Such a ferromagnetic effect (discovered in the pioneering works[33−35]) is rather general due to its distinct physical origin and is well-established in MV dimers and square-planar MV tetramers comprising one excess electron or hole (an exclusion is represented by the effect of frustration in MV systems discovered in ref 54, which requires special discussion). That is why the antiferromagnetic effect of the double exchange in a square-planar cluster containing a pair of excess electrons seems to be, at first glance, quite enigmatic.

The physical origin of the antiferromagnetic ground state of the d^2−d^2−d^1−d^1 tetramer has been reasoned in ref 55. As far as this issue is relevant to further consideration, we repeat the arguments in a few words. In fact, the spins of the two excess electrons remain completely paired in course of the electron delocalization in a bielectronic MV subunit d^1−d^1−d^0−d^0 in which the two electrons are delocalized among four diamagnetic sites (see refs 56 and 57). Therefore, the electron that keeps its spin "up" tends to polarize the core spins also "up", while the second electron with spin "down" produces the opposite effect. This results in full compensation of the magnetic moments of the four spins because the two spin cores have spin "up" and the remaining two are with spin "down", as illustrated in Figure 2b. One can see that the effect of the double exchange in a many-electron system is not always ferromagnetic although the underlying polarization mechanism of spin cores is ferromagnetic.

3.2. Further Computational Details: Effective Hamiltonian in the Strong-*U*-Approximation. We will focus on the most topical case when the ground Coulomb manifold is separated from the excited manifold (Figure 1) by the Coulomb gap, which considerably exceeds the transfer parameter t and the exchange parameters $J_{n,n}$, $J_{n+1,n}$, and $J_{n+1,n+1}$. In this case, which will be referred to as the strong-U -limit, one can apply the perturbation theory with the Coulomb term $\hat{H}_0$ playing the role of the zero-order Hamiltonian and the operator $\hat{V}$ acting as perturbation. Up to the second order, one obtains the following effective Hamiltonian $\hat{H}_{\text{eff}}^{\text{free cell}} \equiv \hat{W}_0$ operating within the ground Coulomb manifold of the free cell:

$$\hat{W}_0 = \hat{P}_0\hat{V}\hat{P}_0 - \hat{P}_0\hat{V}\hat{P}_1\hat{V}\ \hat{P}_0/U$$
$$= \hat{P}_0\hat{H}_{\text{HDVV}}\hat{P}_0 - \hat{P}_0\hat{H}_{\text{DE}}\hat{P}_1\hat{H}_{\text{DE}}\hat{P}_0/U \quad (8)$$

where $\hat{P}_0$ and $\hat{P}_1$ are the projection operators onto the ground and excited manifolds separated by the Coulomb gap $U \equiv U_{i,i+1} - U_{i,i+2}$. It has been taken into account that $\hat{P}_0\hat{H}_{DE}\hat{P}_0 = 0$ because one-electron transfer transforms a low-lying antipodal configuration into an excited one and thus annihilates the system in the ground manifold. The term $\hat{P}_0\hat{H}_{HDVV}\hat{P}_0$ involves the only exchange interaction that is described by the integral $J_{n+1,n}$ because in the ground Coulomb manifold the occupancies of the i-th and $(i + 1)$-th sites alternate. We will use the short notation $J_{n+1,n} \equiv J$. Then, one can write the term $\hat{P}_0\hat{H}_{HDVV}\hat{P}_0$ as follows:

$$\hat{P}_0\hat{H}_{\text{HDVV}}\hat{P}_0 = -2J(\hat{O}_{1\,3} + \hat{O}_{24})\hat{S}_{13}\hat{S}_{24} \quad (9)$$

where $\hat{S}_{13} = \hat{S}_1 + \hat{S}_3$ and $\hat{S}_{24} = \hat{S}_2 + \hat{S}_4$ are the spin operators for the two diagonal local spin dyads. Using the Kambe method,[58] we present the scalar product in eq 9 in the following form:

$$\hat{S}_{13}\hat{S}_{24} = \frac{1}{2}(\hat{S}^2 - \hat{S}_{13}^2 - \hat{S}_{24}^2) \quad (10)$$

Then, each of the two diagonal distributions k,l = 1, 3 and 2, 4 (for the sake of brevity, we will denote these two distributions as D_1 and D_2) gives rise to the following eigenvalues of the operator $\hat{P}_0\hat{H}_{\text{HDVV}}\hat{P}_0$:

$$E_{k,l}(S_{13}, S_{24}, S) = -J[S(S + 1) - S_{13}(S_{13} + 1)$$
$$- S_{24}(S_{24} + 1)] \quad (11)$$

which depend on the two intermediate spins S_{13} and S_{24} (the allowed values of these intermediate spins are of course dictated by the electronic distribution k,l) and the total spin S. The term $\hat{P}_0\hat{H}_{DE}\hat{P}_1\hat{H}_{DE}\hat{P}_0/U$ in eq 8 represents the second-order double-exchange Hamiltonian. It acts within the groups of states belonging to each of the two diagonal distributions D_1 and D_2 and also mixes these two groups of states. It is evident that

$$\hat{H}_{\text{DE}}^{(2)} = -\hat{P}_0\hat{H}_{\text{DE}}\hat{P}_1\hat{H}_{\text{DE}}\hat{P}_0/U \propto t^2/U \quad (12)$$

where $t^2/U \equiv \tau$ can be regarded as a parameter of the second-order double exchange. One can see that under the condition of strong Coulomb repulsion the double exchange is strongly reduced by the factor $|t|/U$.

3.3. Working Cell in the Coulomb Field of the Driver Cell. In QCA, a definite cell ("working cell" or cell **1**) is subjected to the action of the electrostatic quadrupole Coulomb field induced by the polarized neighboring "driver cell" (cell **2**). The Hamiltonian of the working cell in the

https://dx.doi.org/10.1021/acs.jpcc.0c08186
J. Phys. Chem. C 2020, 124, 25602−25614

electrostatic field $\hat{H}_{\text{eff}}^{\text{cell}-\text{cell}} \equiv \hat{W}_{\text{cc}}$ of the driver cell is the following:

$$\hat{W}_{\text{cc}} = \hat{W}_0 + \hat{H}_{\text{QF}} \tag{13}$$

The first term in eq 13 is the effective second-order Hamiltonian of the free cell obtained within the strong-U-limit and operating within the restricted space of the ground Coulomb manifold, which arise from the distributions D_1 and D_2 of the two electrons when they occupy the remote centers disposed along the diagonals 1−3 and 2−4 of the square (eq 8) and includes the second-order double exchange and the HDVV exchange. The term $\hat{H}_{\text{QF}}$ is defined as follows

$$\hat{H}_{\text{QF}} = \frac{1}{2} u\, P_2(\hat{n}_2 + \hat{n}_4 - \hat{n}_1 - \hat{n}_3) \tag{14}$$

This term describes the interaction of the working cell with the quadrupole Coulomb field of the driver cell. In eq 14, u is the parameter of the intercell Coulomb interaction (explicitly defined as in refs 59 and 60) and $\hat{n}_i$ is the excess electron occupation operator for the site i. The value P_2 is the driver-cell polarization, which in the strong-U-limit is defined as follows

$$P_2 = \frac{\rho'_{13} - \rho'_{24}}{\rho'_{13} + \rho'_{24}} \tag{15}$$

In eq 15, ρ'_{13} and ρ'_{24} are the probabilities (or alternatively, electronic densities) of the two diagonal localizations of the electronic pair in the driver cell. Note that the strong-U-limit implies the normalization condition, which can be expressed as $\rho'_{13} + \rho'_{24} = 1$. It is assumed that P_2 can be varied in a controllable manner from the fully polarized state with $P_2 = -1$ ($\rho'_{13} = 0$, $\rho'_{24} = 1$) to the fully polarized state with $P_2 = +1$ ($\rho'_{13} = 1$, $\rho'_{24} = 0$) passing through the unpolarized fully delocalized state with $P_2 = 0$ in which the electronic pair is equally distributed over two diagonal positions ($\rho'_{13} = \rho'_{24} = 1/2$).

Eigenvalues of the Hamiltonian, $\hat{W}_{\text{cc}} = \hat{W}_0 + \hat{H}_{\text{QF}}$, as functions of the parameters J, τ, and u and of the driver-cell polarization P_2 are given in Table 1. The ground spin-states of a free cell ($P_2 = 0$) found for three different ranges of $|J|/\tau$ (J <0) are given in Table 2. Discussion of these dependences will be given in a subsequent section.

3.4. Energies of the Isolated Six-Electron Tetrameric Square-Planar Cell. For diagonal distributions D_1 and D_2 within the adopted spin-coupling scheme S_{13}, S_{24}, and S, we obtain two states with $S = 3$, six states with $S = 2$, eight states with $S = 1$, and four states with $S = 0$. These states are listed in Table 1, which gives also the energies of a free cell (that are eigenvalues at $P_2 = 0$). The ground spin-states of a free cell in different ranges of the ratio $|J|/\tau$ providing $J < 0$ are given in Table 2.

In the general case when both J and t are nonzero, the effect of the second-order double exchange $\hat{H}_{\text{DE}}^{(2)}$ on the energy levels is specific for different states. It is seen from Table 1 that in some cases double exchange does not mix the states with the same S, which are obtained from each other by changing $D_1 \rightleftarrows D_2$ and $S_{13} \rightleftarrows S_{24}$, but only shifts their energies giving rise to a deviation from the eigenvalues of the HDVV scheme. Such a situation occurs for the following $|D_i, S_{13}, S_{24}, S\rangle$-states: $|D_1, 2, 1, 3\rangle$, $|D_2, 1, 2, 3\rangle$, $|D_1, 2, 1, 2\rangle$, $|D_2, 1, 2, 2\rangle$, $|D_1, 2, 0, 2\rangle$, $|D_2, 0, 2, 2\rangle$, $|D_1, 2, 1, 1\rangle$, $|D_2, 1, 2, 1\rangle$. For all other pairs of states belonging to different distributions with the same spin quantum numbers, the double exchange in addition to equal shifts of the two levels also produces mixing of states belonging to different distributions. Thus, for example, the eigenvalues $-(4J + 11\tau)/2$ and $-(4J + 3\tau)/2$ correspond to the mixed states $(|D_1, 1, 1, 2\rangle \pm |D_2, 1, 1, 2\rangle)\sqrt{2}$ possessing opposite parities.

Table 1. Energies of the Tetrameric Molecular Square Cell of d^2−d^2−d^1−d^1-Type Evaluated in the Strong-U-Limit as Functions of J, τ, u, and P_2[a]

distribution	S_{13}	S_{24}	S	Energies
D_1	2	1	3	$-4J - 4\tau - uP_2$
D_2	1	2	3	$-4J - 4\tau + uP_2$
D_1	2	1	2	$(4J - 5\tau - 2uP_2)/2$
D_2	1	2	2	$(4J - 5\tau + 2uP_2)/2$
D_1	2	0	2	$-3\tau - uP_2$
D_2	0	2	2	$-3\tau + uP_2$
D_1	1	1	2	$(-4J - 7\tau \pm 2\sqrt{4\tau^2 + u^2P_2^2})/2$
D_2	1	1	2	
D_1	2	1	1	$(12J - 3\tau - 2uP_2)/2$
D_2	1	2	1	$(12J - 3\tau + 2uP_2)/2$
D_1	1	1	1	$(4J - 5\tau \pm 2\sqrt{4\tau^2 + u^2P_2^2})/2$
D_2	1	1	1	
D_1	1	0	1	$-3\tau \pm \sqrt{6\tau^2 + u^2P_2^2}$
D_2	1	0	1	
D_1	0	1	1	$-3\tau \pm \sqrt{6\tau^2 + u^2P_2^2}$
D_2	0	1	1	
D_1	1	1	0	$4J - 2\tau \pm \sqrt{4\tau^2 + u^2P_2^2}$
D_2	1	1	0	
D_1	0	0	0	$-3\tau \pm \sqrt{9\tau^2 + u^2P_2^2}$
D_2	0	0	0	

[a]The electronic distributions D_i, intermediate spins S_{13}, S_{34}, and the total spin S specifying full spin states are indicated.

Table 2. Ground Spin-States of a Free Cell ($P_2 = 0$) in Different Ranges of the Ratio $|J|/\tau$ Provided That $J < 0$

(D_i, S_{13}, S_{24}, S)	ground-state energy	condition
$(D_1, 2, 1, 1)$, $(D_2, 1, 2, 1)$	$(1/2)\ (12J - 3\tau)$	$\lvert J\rvert/\tau > 5/4$
$(D_2, 1, 1, 0)$, $(D_2, 1, 1, 0)$	$4J - 4\tau$	$1/2 < \lvert J\rvert/\tau < 5/4$
$(D_1, 0, 0, 0)$, $(D_2, 0, 0, 0)$	-6τ	$\lvert J\rvert/\tau < 1/2$

The energies as functions of J and τ are shown in the correlation diagram (Figure 3). It is seen that depending on the relative values of J and τ the ground state can be either diamagnetic ($S = 0$) or paramagnetic with $S = 1$ (Table 2). For the case of a relatively weak second-order double exchange defined by inequality $|J|/\tau > 5/4$, the ground state is an orbital doublet with $S = 1$ having two components $|D_1, 2, 1, 1\rangle$ and $|D_2, 1, 2, 1\rangle$. For $1/2 < |J|/\tau < 5/4$ (moderate second-order double exchange), the ground state is a spin-singlet containing equal contributions of the two localized states $|D_1, 1, 1, 0\rangle$ and |

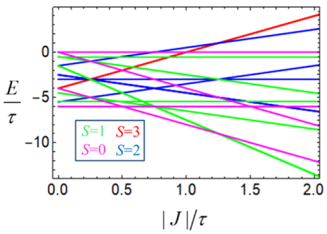

Figure 3. Correlation diagram for the isolated cell representing the square-planar d^2−d^2−d^1−d^1-tetramer calculated within the strong-U-limit. Coloring of spin states is shown in the inset.

https://dx.doi.org/10.1021/acs.jpcc.0c08186
J. Phys. Chem. C 2020, 124, 25602−25614

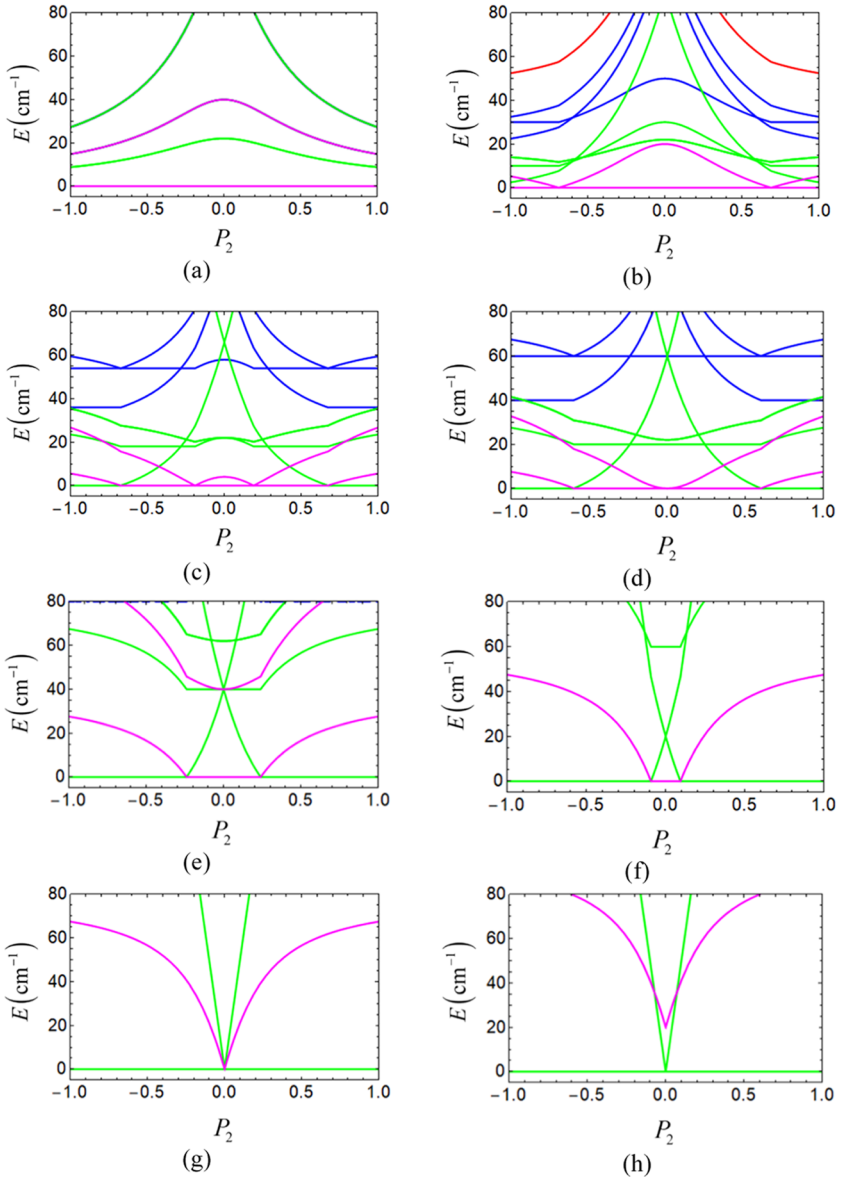

Figure 4. Low-lying energy levels of the tetrameric square cell of $d^2-d^2-d^1-d^1$-type calculated as functions of driver-cell polarizations P_2 with u = 250 cm^{-1}, τ = 40 cm^{-1}, and J = −10 cm^{-1} (a), −15 cm^{-1} (b), −19 cm^{-1} (c), −20 cm^{-1} (d), −30 cm^{-1} (e), −40 cm^{-1} (f), −50 cm^{-1} (g), and −60 cm^{-1} (h). Here and in the subsequent two figures, the same coloring as in Figure 3 is used and the ground-state energy level is chosen as a reference one.

D_2, 1, 1, 0⟩. Finally, for $|J|/\tau < 1/2$ (case of a strong second-order double exchange), the ground state is the other spin-singlet in which the two localized states $|D_1$, 0, 0, 0⟩ and $|D_2$, 0, 0, 0⟩ are present with equal weights.

3.5. Working Cell in the Field of the Driver Cell and Spin-Switching. The eigenvalues of the Hamiltonian, eq 13, as functions of the driver-cell polarization P_2 are given in Table 1. To rationalize the results, it is worth referring to the concept of the group-theoretical assignation of the spin multiplets,[61−63] which provides us with the interrelation between the eigenstates of the model $t-J$-Hamiltonian and exact terms of the systems enumerated by the irreducible representations of the point group and full spins. Here, we need only restricted information from the group-theoretical assignation of the free cell states that allows us to qualitatively distinguish the state of the system according to their polarizability by the driver's field. For example, one can see (Table 1) that there are two S = 3 levels with (S_{13}, S_{24}) = (1, 2) and (2, 1), which obviously form the orbital doublet ^7E. Alternatively, one can find two spin-singlets having opposite parities with respect to inversion as states with $S_{13} = S_{24} = 0$ and $S_{13} = S_{24} = 1$.

It is seen that the operator of the quadrupole field linearly splits the orbital doublets into two components (e.g., the orbital doublet ^7E is split into orbital singlets $|D_1$, 2, 1, 3⟩ and $|D_2$, 1, 2, 3⟩). This odd operator also mixes pairs of orbital singlets (having different energies) of opposite parities giving rise to a quadratic Stark effect provided that the second-order double-exchange splitting considerably exceeds the Coulomb energy gap $2u|P_2|$ resulting from the cell−cell interaction. Thus, one can distinguish two kinds of pairs of the levels: (1) the pairs exhibiting the linear Stark effect and (2) those for which this effect is quadratic. The levels exhibiting linear dependence of uP_2 represent fully localized states arising from the two components of the free cell orbital doublets, with each

https://dx.doi.org/10.1021/acs.jpcc.0c08186
J. Phys. Chem. C 2020, 124, 25602−25614

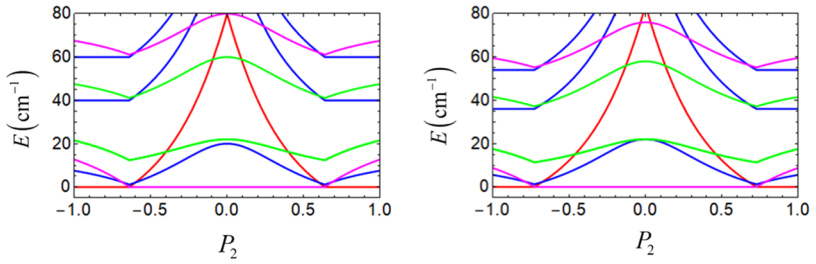

Figure 5. Low-lying energy levels of the tetrameric square cell of d^2−d^2−d^1−d^1-type calculated as functions of driver-cell polarizations P_2 with u = 250 cm^{-1}, τ = 40 cm^{-1}, and J = 0 (a) and −1 cm^{-1} (b).

component having a definite electronic distribution. On the contrary, the states whose energies depend on uP_2 nonlinearly prove to be delocalized, and therefore the system in these states has lower polarizability under the action of the driver cell.

Now let us discuss the influence of the driver's field on the system in the three topical cases of the ground states listed in Table 2 and shown in Figure 3, namely, spin-triplet and two spin-singlets. First of all, let us note that the spin-triplet, which is a ground state at weak or zero double exchange, should exhibit strong linear Stark splitting (according to the above discussion), while the two spin-singlets (the state with $S_{13} = S_{24} = 0$ and that with $S_{13} = S_{24} = 1$) demonstrate quadratic Stark effect and hence undergo weaker stabilization by the intercell Coulomb field. This means that the intercell Coulomb field tends to stabilize the spin-triplet with respect to both these spin-singlets. On the other hand, by comparing the two spin-triplets, one can see that at $P_2 = 0$ the two states of opposite parities having $S_{13} = S_{24} = 0$ are separated by the larger double-exchange energy gap of 6τ than the corresponding two states with $S_{13} = S_{24} = 1$ (energy gap of 4τ). For this reason, the two states of opposite parities with $S_{13} = S_{24} = 1$ are stronger mixed by the intercell Coulomb field than the two states having $S_{13} = S_{24} = 0$, and hence such fields tend to stabilize the low-lying spin-singlet with $S_{13} = S_{24} = 1$ with respect to the spin-singlet possessing $S_{13} = S_{24} = 0$.

Due to different polarizabilities of the above three spin-states, one can expect that under some conditions the field created by the polarized driver cell can induce switching between these states. This expectation is confirmed by the dependences of the energy levels of the working cell on the polarization of the driver cell calculated at fixed values of the second-order double exchange τ = 40 cm^{-1}, intercell Coulomb energy u = 250 cm^{-1}, and different parameters J of HDVV exchange. These dependences are shown in Figure 4a−h.

It is worth noting that the used values of the parameters τ and J prove to be of the same order of magnitude as the spin−orbit coupling parameters for the metals of 3d series. Nevertheless, as was mentioned, the present model of the cell does not include the spin−orbit coupling, which is assumed to be reduced by the low-symmetry crystal field. Under this condition, the spin−orbit coupling in such systems only acts as a second-order contribution, which plays quite an insignificant role in the effects we discuss here.

Figure 4a shows the case of relatively strong double exchange $|J|/\tau = 1/4$ when at $P_2 = 0$ the ground state is the spin-singlet with $S_{13} = S_{24} = 0$. It is seen that this state remains the ground one even at extremely strong polarization of the driver cell (i.e., at $P_2 = \pm 1$) although the energy gap between this state and the excited states with $S = 0$ and 1 is diminished. For weaker (the case of $|J|/\tau = 3/8$ in Figure 4b) but still strong double exchange satisfying the inequality $|J|/\tau < 1/2$, the ground state of the free cell is the same spin-singlet with $S_{13} = S_{24} = 0$ as that in Figure 4a, but the energy gap between this state and the excited spin-singlet with $S_{13} = S_{24} = 1$ is strongly reduced. Due to that, for a strong-enough Coulomb field (at $P_2 \approx \pm 0.7$), the ground state undergoes switching from the spin-singlet possessing $S_{13} = S_{24} = 0$ to the spin-singlet with $S_{13} = S_{24} = 1$. It is also seen from Figure 4b that the excited spin-triplet level approaches the ground spin-singlet level upon the increase of the driver-cell polarization. This is because, as we have mentioned above, the $S = 1$ state of the working cell possesses a higher sensitivity to the Coulomb field induced by the driver cell (linear Stark effect) as compared with the $S = 0$ state for which the Stark effect is quadratic. Further decrease of the relative strength of double exchange (Figure 4c) leads to the decrease of the critical value of the driver-cell polarization required for switching between the two spin-singlet states and also (at stronger driver-cell polarization) to spin-switching from the spin-singlet with $S_{13} = S_{24} = 1$ to the spin-triplet, which can be either the $|D_1, 2, 1, 1\rangle$ or $|D_2, 1, 2, 1\rangle$ state depending on the sign of P_2.

Figure 4d shows the special case when $|J|/\tau = 1/2$ (borderline between the cases of strong and moderate double exchange) for which at $P_2 = 0$ the two spin-singlets possess the same energy and form the ground state that is an orbital doublet with $S = 0$. The quadrupole field of the driver cell splits this orbital doublet in such a way that the ground state proves to be spin-singlet with $S_{13} = S_{24} = 1$. Then, at $P_2 \approx \pm 0.6$, the cell undergoes spin-switching from the spin-singlet to the spin doublet.

Subject to moderate double exchange, the Coulomb field of the driver cell can induce only one switching event, which occurs with the change of the spin from $S = 0$ ($S_{13} = S_{24} = 1$) to $S = 1$ (Figure 4e,f). By comparing Figure 4e,f, one can see that the weaker is double exchange (larger ratio $|J|/\tau$), the narrower is the range of P_2 for which the ground state is the spin-singlet, until at $|J|/\tau = 5/4$ (borderline between the cases of moderate and weak double exchange) this range is reduced to the only point ($P_2 = 0$) in which the ground state represents a paramagnetic mixture of spin-singlet and spin-triplet. This borderline case is shown in Figure 4g.

Finally, the case of weak double exchange is shown in Figure 4h. It is seen that the ground state is a spin-triplet for all values of polarization of the driver cell, namely, at $P_2 = 0$ it is an orbital doublet comprising two components $|D_1, 2, 1, 1\rangle$ and $|D_2, 1, 2, 1\rangle$, while for $P_2 \neq 0$ it is one of the orbital singlets ($|D_1, 2, 1, 1\rangle$ or $|D_2, 1, 2, 1\rangle$) depending on the sign of P_2.

https://dx.doi.org/10.1021/acs.jpcc.0c08186
J. Phys. Chem. C 2020, 124, 25602−25614

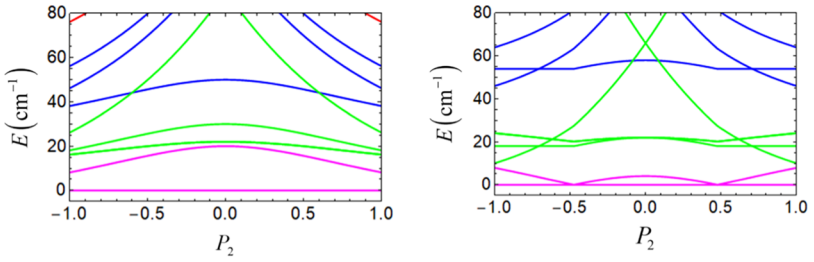

Figure 6. Low-lying energy levels of the tetrameric square cell of $d^2-d^2-d^1-d^1$-type calculated as functions of driver-cell polarizations P_2 with u = 100 cm^{-1}, τ = 40 cm^{-1}, and J = −15 cm^{-1} (a) and −19 cm^{-1} (b). Coloring is the same as in Figure 2. The ground-state energy level is chosen as a reference one.

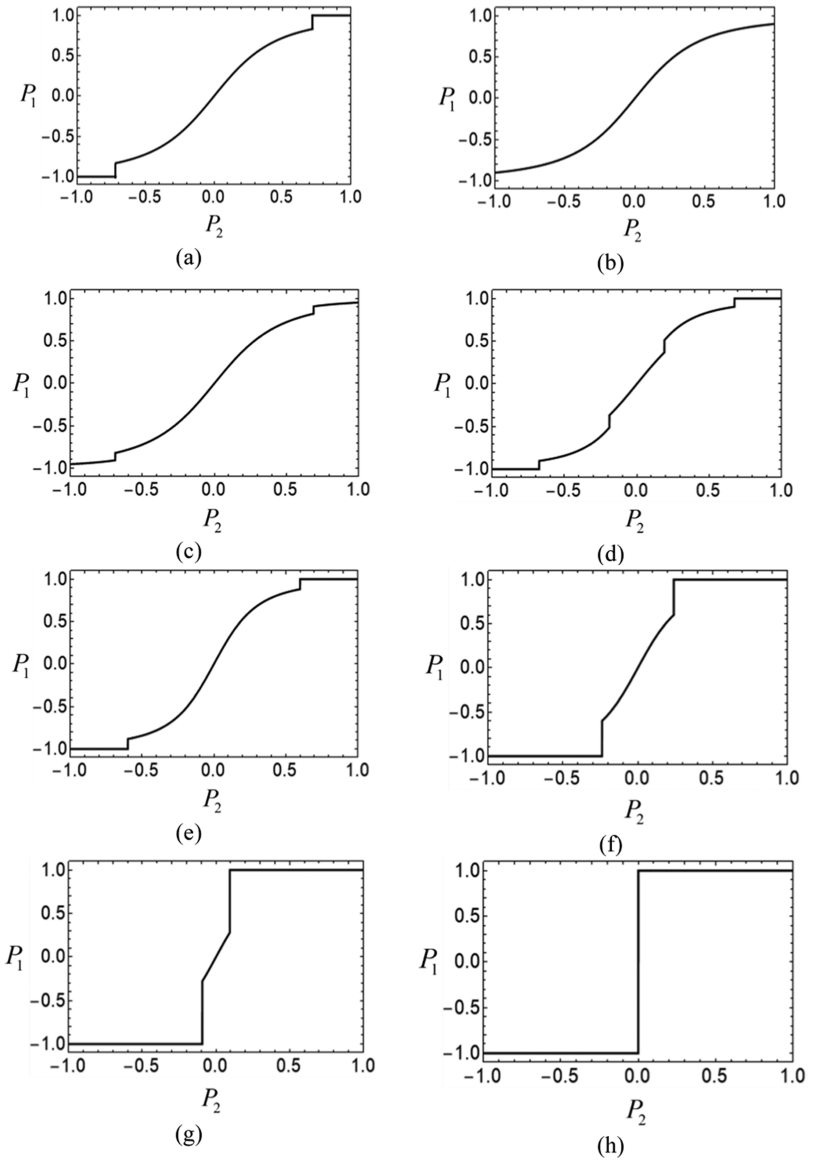

Figure 7. Cell−cell response functions for the tetrameric square cell of $d^2-d^2-d^1-d^1$-type calculated as functions of driver-cell polarizations P_2 with u = 250 cm^{-1}, τ = 40 cm^{-1}, and the following values of J: −1 cm^{-1} (a), −10 cm^{-1} (b), −15 cm^{-1} (c), −19 cm^{-1} (d), −20 cm^{-1} (e), −30 cm^{-1} (f), −40 cm^{-1} (g), and −50 cm^{-1} (h).

Up to now, we have discussed the cases when the ground state of the working cell subjected by the electrostatic field induced by the fully polarized driver cell ($|P_2| = 1$) is one of the spin states that can be the ground states also at zero field ($P_2 = 0$). Now we will consider a special case when at large $|P_2|$ the cell proves to be switched into the spin state that can never be a ground state at $P_2 = 0$. This is a case of extremely strong (as compared with the HDVV exchange) double exchange, which

https://dx.doi.org/10.1021/acs.jpcc.0c08186
J. Phys. Chem. C 2020, 124, 25602−25614

is illustrated for $J = 0$ (Figure 5a) and $J = -1$ cm^{-1} (Figure 5b) provided that $\tau = -40$ cm^{-1}. One can see that in such a case the quadrupole field induces switching from the state with $S = 0$ to that having $S = 3$ (the latter state exhibits a linear Stark effect). The appearance of the state with $S = 3$ as a ground state at a strong quadrupole field proves to be possible due to the fact that the energy spectrum of the fully polarized working cell is in general different from the spectrum obtained in the HDVV limit in which the ground state is always the spin-triplet. This is because the quadrupole field only partially reduces the second-order double exchange, namely, only the terms mixing the electronic distributions D_1 and D_2 are suppressed by the field, while the terms acting within each electronic distribution remain unaffected. The latter terms lead to the deviation of the energy spectrum of the cell in the strong field limit from that produced by HDVV exchange only. As a result, the fully polarized working cell is shown to possess the ground state with $S = 3$ at $|J|/\tau < 1/4$ and just this state is stabilized by the field in the case of very strong second-order double exchange (Figure 5a,b). The possibility to induce such a strong change in the spin is quite attractive for designing spin-switching devices.

In the above model calculations, we have fixed the intercell Coulomb energy u, which is mainly determined by the geometric factors (dimension of the square cell and the intercell distance). This has allowed us to answer the question on how the relative strength of the two electronic interactions acting in the cell (second-order double exchange and HDVV exchange) influences the features of the energy spectra and the switching conditions. Now, let us briefly examine how the intercell Coulomb energy affects the energy spectra of the working cell, by plotting energy spectra of the working cell evaluated with the same sets of τ and J values, as those in Figure 4b,c, but with twice smaller u. The cases of smaller u are shown in Figure 6a,b. It is seen that as distinguished from the case shown in Figure 4b, in the case presented in Figure 6a, the field created by the driver cell can only reduce the gap between the ground spin-singlet with $S_{13} = S_{24} = 0$ and the excited spin-singlet with $S_{13} = S_{24} = 1$, but it is too low (even at fully polarized driver cell when $P_2 = \pm 1$) to produce switching between these two states. To induce such switching, one needs stronger HDVV exchange (see Figure 6b), but unlike the case shown in Figure 4c when the two switching events occur (switching without the change of S at weak polarization of the driver cell and spin-switching at strong such polarization), Figure 6b evidences only switching between the two spin-singlets. Indeed, it is seen that although the excited spin-triplet is strongly stabilized the quadrupole field is not strong enough (even provided that the driver cell is fully polarized) to make this state the ground one. Again, to achieve spin-switching at this value of the parameter u, the HDVV exchange should be stronger than that in Figure 6b (this case is not shown in the plot). Therefore, switching conditions are substantially dependent on the strength of the intercell Coulomb field.

3.6. Cell−Cell Response Function. Under certain interrelations between the parameters of the double exchange and the HDVV exchange, one can observe crossover between different spin states of the system that results also in a considerable change of the electric polarizability of the cell. Using the expression for the working cell, one can evaluate its dependence of the induced polarization of the working cell P_1 on the polarization of the driver cell P_2, i.e., the cell−cell response, which is a key characteristic of the molecular cell. To describe these characteristics, we show in Figure 7a−h a series of cell−cell response functions evaluated at different parameters of the model. For the sake of simplicity, we will focus on the case of the zero-temperature limit when the working cell is in the ground state.

Figure 7a relates to the case of strong double exchange essentially exceeding the HDVV exchange. In this case at $P_2 = 0$, the ground state is the spin-singlet and at some critical value of P_2 the total spin changes from $S = 0$ to 3. This spin-switching is accompanied by the discontinuous change of P_1, which immediately reaches its saturation value +1 or −1 corresponding to the fully polarized working cell.

For weaker but still strong double exchange showing the ground state at $P_2 = 0$ is the spin-singlet having $S_{13} = S_{24} = 0$ independent of P_2, and this state shows a relatively weak (quadratic at low field) Stark effect or, in other words, this state is weakly sensitive to the field of the driver cell. As a result, the cell−cell response curve shows a rather gradual behavior (Figure 7b), which is an unfavorable condition for successful functioning of the cell in QCA devices. Indeed, the main requirement for the possibility to use a molecule as a cell is the abrupt nonlinear cell−cell response function (see, for example, refs 5 and 6) that is not evidently the case shown in Figure 7b. It is worth noticing, however, that the case of strong double exchange (as compared with the HDVV exchange) cannot be regarded as a case fully excluding the ability of the tetramer to work as an efficient cell. To clarify this point, in Figure 8 we have shown three cell−cell response curves

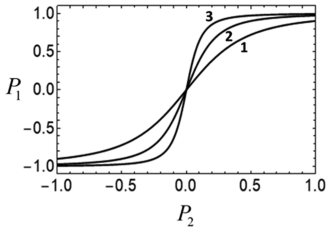

Figure 8. Cell−cell response functions for the tetrameric square cell of d^2−d^2−d^1−d^1-type calculated as functions of driver-cell polarizations P_2 with $u = 250$ cm^{-1} and the following three sets of t^2/U and J values, which keep the ratio $|J|\tau = 1/4$: $\tau = 40$ cm^{-1}, $J = -10$ cm^{-1} (curve **1**); $\tau = 20$ cm^{-1}, $J = -5$ cm^{-1} (curve **2**); and $\tau = 10$ cm^{-1}, $J = -2.5$ cm^{-1} (curve **3**).

evaluated at three different sets of τ and J values preserving at the same time the relative strength of the double exchange and HDVV exchange interactions corresponding to the case of strong double exchange. The ratio $|J|/\tau = 1/4$ used in all cases shown in Figure 8 is the same as in Figure 7b; moreover, curve 1 in Figure 8 is the same curve as that shown in Figure 7b.

The slope of the cell−cell response function strongly depends on the interrelation between the values of τ and J. Actually, at smaller values of τ, the slope of the cell−cell response function is larger and hence better performance of the tetramer as a cell can be expected. One can thus conclude that even in the case of strong double exchange the cluster can be used as a cell, provided that the parameter τ is smaller (or comparable) than the Stark energy at weak polarization of the driver cell. At smaller parameter τ (but still satisfying the condition of strong double exchange), the cell−cell response at weak driver-cell polarization behaves as in the above-considered case, but at some critical value of P_2, it undergoes a nonmonotonic (stepwise) increase (Figure 7c) correspond-

https://dx.doi.org/10.1021/acs.jpcc.0c08186
J. Phys. Chem. C 2020, 124, 25602−25614

ing to the change of the ground state from the spin-singlet with $S_{13} = S_{24} = 0$ to the spin-singlet with $S_{13} = S_{24} = 1$. The latter (as has been discussed) is more sensitive to the field acting on the working cell, and just this difference in the electric polarizabilities of the two spin-singlets leads to the abrupt change of P_1 shown in Figure 7c.

The case shown in Figure 7d is characterized by the widest diversity of the ground states and corresponding electric polarizabilities. As far as the inequality $|J|/\tau < 1/2$ related to the case of strong double exchange is still satisfied, the ground state of the working cell at weak polarization of the driver cell is the spin-singlet with $S_{13} = S_{24} = 0$ and hence the function $P_1(P_2)$ in this range of P_2 values shows a gradual behavior (see above Section 3). Then, at $P_2 \approx \pm 0.2$, the cell−cell response function undergoes the first stepwise change associated with the change of the ground state, which occurs without the change of S. Finally, at $P_2 \approx \pm 0.7$, the second abrupt change of P_1 occurs, which corresponds to spin-switching from the spin-singlet with $S_{13} = S_{24} = 1$ to the spin-triplet. In course of this second jump, the working cell becomes fully polarized.

Plots in Figure 7e−g relate to the case of moderate double exchange in which at P_2 the ground state is the $S = 0$ state with $S_{13} = S_{24} = 1$, and at some critical value of P_2, the total spin changes to $S = 1$. As a result, $|P_1|$ changes abruptly to its saturation value $|P_1| = 1$.

From a comparison of Figure 6d−f, one can see that the larger the $|J|/\tau$ ratio is, the lower is the Coulomb field required to cause the jump of P_1. Finally, at weak double exchange (Figure 7h), the ground state is a spin-triplet independent of P_2. Since this state is very sensitive to the intercell electrostatic field (spin-triplet exhibits a linear Stark effect), even very weak such fields lead to full polarization of the working cell.

In conclusion of the discussion of the cell−cell response function, the following remark should be made concerning the class of the QCA cell under consideration. The ability of the cell to change its magnetization under cell−cell interactions makes these systems somewhat similar to the magnetic QCA in which the binary **0** and **1** are encoded in the two different spin states of the cell ("spin-up" and "spin-down"). Note, however, that the considered QCA still represents the charge-transfer QCA rather than the magnetic QCA because (i) the charge distributions (polarizations) rather than magnetization directions are used to encode binary information and (ii) the intercell electrostatic field rather than the intercell magnetic interactions (intercell exchange, etc.) is used as a driving force causing the switching of the cell between **0** and **1**. On the other hand, as distinguished from the traditional charge-transfer QCA composed of the two-electron square cells, the properties of the multielectron charge-transfer QCA considered here are essentially influenced by the involvement of the spin degrees of freedom arising from the two magnetic intracell interactions, which are the double exchange and the HDVV exchange. From this point of view, the case of relatively strong double exchange shown in Figures 7b and 8 when the spin-singlet with $S_{13} = S_{24} = 0$ remains the ground state of the working cell independent of the polarization of the driver cell and the cell−cell response function is monotonic can be regarded as a limiting case, when the considered QCA behaves as a traditional charge-transfer QCA in which only the charge degrees of freedom are in the game.

4. CONCLUSIONS

We have demonstrated that the multielectron MV molecules exhibiting double exchange may be used to create functioning cells for QCA. It has been shown that these systems can provide additional functionality coming from the combined exploration of spin degrees of freedom and double exchange, such as spin-switching caused by the electric field of the driver cell. We have analyzed the energy levels of isolated and interacting square-planar cells represented by the MV transition-metal tetramers of $d^2-d^2-d^1-d^1$ type or similar tetramers based on quantum dots and also the cell−cell response in such systems.

It has been shown that the double exchange tends to stabilize the spin-singlet ground state of the isolated cell. This result seemingly contradicting the main concept of the double exchange has been explained in terms of spin-polarization of the spin-core system by the spin-singlet electronic pair. In contrast, the antiferromagnetic HDVV exchange tends to stabilize the spin-triplet of the system. In a topical case of large intracell Coulomb gap U, the ground state of the free cell has been shown to be either a spin-triplet or one of the two kinds of spin-triplets with different extents of electron delocalization depending on the relative strength of the HDVV exchange and the second-order double exchange.

For interacting cells, it has been demonstrated that under some conditions the electrostatic field induced by the polarized driver cell can induce spin-switching between the different spin states. The most pronounced spin-switching has been shown to occur when the double exchange is extremely strong as compared with the HDVV exchange. In the latter case, the spin-switching leads to the change of S from $S = 0$ to 3. In other cases, less-pronounced spin-switching from $S = 0$ to 1 has been predicted. Also, switching between the two different spin-singlets has been shown to be possible. In all of these cases, the cell−cell response functions have been shown to behave nonmonotonically due to the fact that different spin states exhibit different polarizabilities with respect to the quadrupole field induced by the driver cell. Finally, the possibility to observe monotonic cell−cell response has also been indicated for the cases of the field-independent ground state. In the latter cases, the spin degrees of freedom can be ruled out from the consideration and the behavior of the QCA considered here proves to be quite similar to that reported earlier for more traditional charge-transfer QCA composed of two-electron square-planar cells.

Therefore, the above analysis has allowed us to go beyond QCA based on cells in which the excess electrons are delocalized over the diamagnetic (spinless) cores and to propose the usage of multielectron MV molecules or multielectron square arrays of quantum dots with competing double exchange and HDVV exchange for the creation of QCA cells. This is expected to considerably extend the class of systems suitable for QCA design and to supply the QCA-based devices with new useful functions, such as spin-switching.

To make the presentation clearer at this stage of the theory, we have intentionally excluded from the consideration the vibronic coupling, which is an important factor of the problem of mixed valency (see refs 56 and 57). This is a conceptually clear task but requires complex calculations. We plan to return to this problem.

It is to be noted that the study carried out is limited by the framework of a semiempirical model theory, which made it

https://dx.doi.org/10.1021/acs.jpcc.0c08186
J. Phys. Chem. C 2020, 124, 25602−25614

possible to formulate general results and relationships between the parameters that are favorable for the functioning of QCA. For further realization of the general concepts, we plan to combine the model study with the computer design and ab initio consideration of the perspective systems. Such a kind of combined parametric/ab initio approach presented in ref 60 proved to be useful.

Finally, the interaction of the molecular system with the environment and the consequent problem of heat release have not been considered here. The last studies in this area[64−67] give reliable tools for the estimation of the heat release in QCA circuits. In this respect, the MV cells containing paramagnetic cores should have essential peculiarities of relaxation that we plan to consider elsewhere on the basis of the quantum-mechanical solution presented in this article.

AUTHOR INFORMATION

Corresponding Authors

Andrew Palii − *Laboratory of Molecular Magnetic Nanomaterials, Institute of Problems of Chemical Physics, Chernogolovka, Moscow Region 142432, Russian Federation*; Email: andrew.palii@uv.es

Juan Modesto Clemente-Juan − *Instituto de Ciencia Molecular, Universidad de Valencia, 46980 Paterna, Spain*; orcid.org/0000-0002-3198-073X; Email: juan.m.clemente@uv.es

Boris Tsukerblat − *Department of Chemical Sciences, Ariel University, 40700 Ariel, Israel; Department of Chemistry, Ben-Gurion University of the Negev, 84105 Beer-Sheva, Israel*; orcid.org/0000-0002-8182-6140; Email: tsuker@bgu.ac.il

Authors

Sergey Aldoshin − *Laboratory of Molecular Magnetic Nanomaterials, Institute of Problems of Chemical Physics, Chernogolovka, Moscow Region 142432, Russian Federation*

Denis Korchagin − *Laboratory of Molecular Magnetic Nanomaterials, Institute of Problems of Chemical Physics, Chernogolovka, Moscow Region 142432, Russian Federation*; orcid.org/0000-0002-0199-1382

Andrey Rybakov − *Laboratory of Molecular Magnetic Nanomaterials, Institute of Problems of Chemical Physics, Chernogolovka, Moscow Region 142432, Russian Federation; Moscow Institute of Physics and Technology, Dolgoprudny, Moscow Region 141701, Russian Federation*; orcid.org/0000-0002-9924-3576

Shmuel Zilberg − *Department of Chemical Sciences, Ariel University, 40700 Ariel, Israel*

Complete contact information is available at: https://pubs.acs.org/10.1021/acs.jpcc.0c08186

Notes

The authors declare no competing financial interest.

ACKNOWLEDGMENTS

A.P., S.A., D.K., E.G., A.R., S.Z., and B.T. acknowledge support from the Russian Science Foundation (project No. 20-13-00374).

REFERENCES

(1) Orlov, A. O.; Amlani, I.; Bernstein, G. H.; Lent, C. S.; Snider, G. L. Realization of a functional cell for quantum-dot cellular automata. *Science* **1997**, *277*, 928−930.

(2) Hänninen, I.; Takala, J. Binary adders on quantum-dot cellular automata. *J. Signal Process. Syst.* **2010**, *58*, 87−103.

(3) Zoka, S.; Gholami, M. A novel rising edge triggered resettable D flip-flop using five input majority gate. *Microprocessors Microsyst.* **2018**, *61*, 327−335.

(4) Zoka, S.; Gholami, M. A novel efficient full adder−subtractor in QCA nanotechnology. *Int. Nano Lett.* **2019**, *9*, 51−54.

(5) Lent, C. S.; Tougaw, P. D.; Porod, W.; Bernstein, G. H. Quantum cellular automata. *Nanotechnology* **1993**, *4*, 49−57.

(6) Lent, C. S.; Tougaw, P.; Porod, W. Bistable saturation in coupled quantum dots for quantum cellular automata. *Appl. Phys. Lett.* **1993**, *62*, 714−716.

(7) Lent, C. S.; Tougaw, P. D. Lines of interacting quantum-dot cells: A binary wire. *J. Appl. Phys.* **1993**, *74*, 6227−6233.

(8) Tougaw, P. D.; Lent, C. S. Logical devices implemented using quantum cellular automata. *J. Appl. Phys.* **1994**, *75*, 1818−1825.

(9) Lent, C. S.; Tougaw, P. D. A device architecture for computing with quantum dots. *Proc. IEEE* **1997**, *85*, 541−557.

(10) Porod, W.; Lent, C. S.; Bernstein, G. H.; Orlov, A. O.; Amlani, I.; Snider, G. L.; Merz, J. L. Quantum-dot cellular automata: Computing with coupled quantum dots. *Int. J. Electronics* **1999**, *86*, 549−590.

(11) Tóth, G.; Lent, C. S. Quasiadiabatic switching for metal-island quantum-dot cellular automata. *J. Appl. Phys.* **1999**, *85*, 2977−2984.

(12) Tóth, G.; Lent, C. S. Quantum computing with quantum-dot cellular automata. *Phys. Rev. A.* **2001**, *63*, No. 052315.

(13) Lent, C. S. Bypassing the transistor paradigm. *Science* **2000**, *288*, 1597−1599.

(14) Hennessy, K.; Lent, C. S. Clocking of molecular quantum-dot cellular automata. *J. Vac. Sci. Technol., B: Microelectron. Process. Phenom.* **2001**, *19*, 1752−1755.

(15) Hush, N. Molecular Electronics: Cool Computing. *Nat. Mater.* **2003**, *2*, 134−135.

(16) Lent, C. S.; Isaksen, B.; Lieberman, M. Molecular quantum-dot cellular automata. *J. Am. Chem. Soc.* **2003**, *125*, 1056−1063.

(17) Jiao, J.; Long, G. J.; Grandjean, F.; Beatty, A. M.; Fehlner, T. P. Building blocks for the molecular expression of quantum cellular automata. isolation and characterization of a covalently bonded square array of two ferrocenium and two ferrocene complexes. *J. Am. Chem. Soc.* **2003**, *125*, 7522−7523.

(18) Li, Z.; Beatty, A. M.; Fehlner, T. P. Molecular QCA Cells. 1. Structure and functionalization of an unsymmetrical dinuclear mixed-valence complex for surface binding. *Inorg. Chem.* **2003**, *42*, 5707−5714.

(19) Li, Z.; Fehlner, T. P. Molecular QCA Cells. 2. Characterization of an unsymmetrical dinuclear mixed-valence complex bound to a au surface by an organic linker. *Inorg. Chem.* **2003**, *42*, 5715−5721.

(20) Qi, H.; Sharma, S.; Li, Z.; Snider, G. L.; Orlov, A. O.; Lent, C. S.; Fehlner, T. P. Molecular quantum cellular automata cells. electric field driven switching of a silicon surface bound array of vertically oriented two-dot molecular quantum cellular automata. *J. Am. Chem. Soc.* **2003**, *125*, 15250−15259.

(21) Braun-Sand, S. B.; Wiest, O. Theoretical studies of mixed valence transition metal complexes for molecular computing. *J. Phys. Chem. A* **2003**, *107*, 285−291.

(22) Braun-Sand, S. B.; Wiest, O. Biasing mixed-valence transition metal complexes in search of bistable complexes for molecular computing. *J. Phys. Chem. B* **2003**, *107*, 9624−9628.

(23) Qi, H.; Gupta, A.; Noll, B. C.; Snider, G. L.; Lu, Y.; Lent, C.; Fehlner, T. P. Dependence of field switched ordered arrays of dinuclear mixed-valence complexes on the distance between the redox centers and the size of the counterions. *J. Am. Chem. Soc.* **2005**, *127*, 15218−15227.

(24) Jiao, J.; Long, G. J.; Rebbouh, L.; Grandjean, F.; Beatty, A. M.; Fehlner, T. P. Properties of a mixed-valence $(Fe^{II})_2(Fe^{III})_2$ Square cell for utilization in the quantum cellular automata paradigm for molecular electronics. *J. Am. Chem. Soc.* **2005**, *127*, 17819−17831.

(25) Lu, Y.; Lent, C. S. Theoretical study of molecular quantum dot cellular automata. *J. Comput. Electron.* **2005**, *4*, 115−118.

(26) Zhao, Y.; Guo, D.; Liu, Y.; He, C.; Duan, C. A Mixed-Valence $(Fe^{II})_2(Fe^{III})_2$ Square for molecular expression of quantum cellular automata. *Chem. Commun.* **2008**, 5725−5727.
(27) Nemykin, V. N.; Rohde, G. T.; Barrett, C. D.; Hadt, R. G.; Bizzarri, C.; Galloni, P.; Floris, B.; Nowik, I.; Herber, R. H.; Marrani, A. G.; et al. Electron-transfer processes in metal-free tetraferrocenylporphyrin. Understanding Internal interactions to access mixed valence states potentially useful for quantum cellular automata. *J. Am. Chem. Soc.* **2009**, *131*, 14969−14978.
(28) Wang, X.; Yu, L.; Inakollu, V. S. S.; Pan, X.; Ma, J.; Yu, H. Molecular Quantum-Dot Cellular Automata Based on Diboryl Radical Anions. *J. Phys. Chem. C* **2018**, *122*, 2454−2460.
(29) *Mixed valency systems: Applications in chemistry, physics and biology, Proceedings of the NATO Advanced Workshop on mixed valency compounds, Aghia Pelaghia, Crete, Greece*, Prassides, K.; Prassides, K., Eds.; D. Reidel Publishing Company: Dordrecht, Boston, London, June 10−16, 1990, NATO ASI Series, Vol. 343.
(30) Blondin, G.; Girerd, J.-J. Interplay of electron exchange and electron transfer in metal polynuclear complexes in proteins or chemical models. *Chem. Rev.* **1990**, *90*, 1359−1376.
(31) Borrás-Almenar, J. J.; Clemente-Juan, J. M.; Coronado, E.; Palii, A. V.; Tsukerblat, B. S. Magnetic Properties of Mixed-Valence Clusters: Theoretical Approaches and Applications. In *Magnetoscience: From Molecules to Materials*; Miller, J.; Drillon, M., Eds.; Villey-VCH, 2001; Vol. 155−210.
(32) Bechlars, B.; D'Alessandro, D. M.; Jenkins, D. M.; Iavarone, A. T.; Glover, S. D.; Kubiak, C. P.; Long, J. R. High-spin ground states via electron delocalization in mixed-valence imidazolate-bridged divanadium complexes. *Nat. Chem.* **2010**, *2*, 362−368.
(33) Zener, C. Interaction between the d-Shells in the Transition Metals. II. Ferromagnetic compounds of manganese with perovskite structure. *Phys. Rev.* **1951**, *82*, 403−405.
(34) Anderson, P. W.; Hasegawa, H. Consideration of double exchange. *Phys. Rev.* **1955**, *100*, 675−681.
(35) De Gennes, P.-G. Effects of double exchange in magnetic crystals. *Phys. Rev.* **1960**, *118*, 141−154.
(36) Kahn, O. *Molecular Magnetism*; Wiley-VCH: New York, 1993.
(37) Bosch-Serrano, C.; Clemente-Juan, J. M.; Coronado, E.; Gaita-Ariño, A.; Palii, A.; Tsukerblat, B. Electric field control of the spin state in mixed-valence magnetic molecules. *Chem. Phys. Chem.* **2012**, *13*, 2662−2665.
(38) Bosch-Serrano, C.; Clemente-Juan, J. M.; Coronado, E.; Gaita-Ariño, A.; Palii, A.; Tsukerblat, B. Molecular analog of multiferroics: electric and magnetic field effects in many-electron mixed-valence dimers. *Phys. Rev. B* **2012**, *86*, No. 024432.
(39) Palii, A.; Tsukerblat, B.; Clemente-Juan, J. M.; Coronado, E. Coherent manipulation of polarization in mixed-valence compounds by electric pulse via Landau-Zener transitions. *J. Phys. Chem. C* **2012**, *116*, 4999−5008.
(40) Suzuki, H.; Satoko, C. Quantitative calculation of magnetic and electric properties in a d^2−d^3 mixed-valence vanadium dimer complex. *J. Phys.: Condens. Matter* **2014**, *26*, No. 045504.
(41) Palii, A.; Clemente-Juan, J. M.; Tsukerblat, B.; Coronado, E. Electric field control of the optical properties in magnetic mixed valence molecules. *Chem. Sci.* **2014**, *5*, 3598−3602.
(42) Palii, A. V.; Clemente-Juan, J. M.; Coronado, E.; Tsukerblat, B. Electric field control of spin-dependent dissipative electron transfer dynamics in mixed-valence molecules. *J. Phys. Chem. C* **2015**, *119*, 7911−7921.
(43) Palii, A.; Aldoshin, S.; Tsukerblat, B.; Clemente-Juan, J. M.; Gaita-Ariño, A.; Coronado, E. Electric field controllable magnetic coupling of localized spins mediated by itinerant electron: a toy model. *Phys. Chem. Chem. Phys.* **2017**, *19*, 26098−26106.
(44) Malinowski, F. K.; Martins, F.; Smith, T. B.; Bartlett, S. D.; Doherty, A. C.; Nissen, P. D. Spin of a multielectron quantum dot and its interaction with a neighboring electron. *Phys. Rev. X* **2018**, *8*, No. 011045.
(45) Beaulac, R.; Archer, P. I.; Ochsenbein, S. T.; Gamelin, D. R. Mn^{2+}-doped CdSe quantum dots: new inorganic materials for spin-electronics and spin-photonics. *Adv. Funct. Mater.* **2008**, *18*, 3873−3891.
(46) Schwartz, D. A.; Norberg, N. S.; Nguyen, Q. P.; Parker, J. M.; Gamelin, D. R. Magnetic quantum dots: synthesis, spectroscopy, and magnetism of Co^{2+}-and Ni^{2+}-doped ZnO nanocrystals. *J. Am. Chem. Soc.* **2003**, *125*, 13205−13218.
(47) Palii, A.; Clemente-Juan, J. M.; Rybakov, A.; Aldoshin, S.; Tsukerblat, B. Exploration of the double exchange in quantum cellular automata: proposal for a new class of cells. *Chem. Commun.* **2020**, *56*, 10682−10685.
(48) Borras-Almenar, J. J.; Clemente-Juan, J. M.; Coronado, E.; Palii, A. V.; Tsukerblat, B. S. Anisotropic double exchange in orbitally degenerate mixed valence systems. *Chem. Phys.* **2000**, *254*, 275−285.
(49) Borrás-Almenar, J. J.; Clemente-Juan, J. M.; Coronado, E.; Georges, R.; Palii, A. V.; Tsukerblat, B. S. High-nuclearity mixed valence clusters: a general solution of the double exchange problem. *J. Chem. Phys.* **1996**, *105*, 6892−6909.
(50) Clemente-Juan, J. M.; Borrás-Almenar, J. J.; Coronado, E.; Palii, A. V.; Tsukerblat, B. S. High-nuclearity mixed-valence clusters and mixed-valence chains: general approach to the calculation of the energy levels and bulk magnetic properties. *Inorg. Chem.* **2009**, *48*, 4557−4568.
(51) Borrás-Almenar, J. J.; Cardona-Serra, S.; Clemente-Juan, J. M.; Coronado, E.; Palii, A. V.; Tsukerblat, B. S. MVPACK: A Package to calculate energy levels and magnetic properties of high nuclearity mixed valence clusters. *J. Comput. Chem.* **2010**, *31*, 1321−1332.
(52) Palii, A. V.; Ostrovsky, S. M.; Tsukerblat, B. S. Double Exchange in Tetrameric Mixed- Valence Clusters. *New J. Chem.* **1992**, *16*, 943−952.
(53) Borras-Almenar, J. J.; Jorge, R.; Klokishner, S. I.; et al. Double exchange in polynuclear mixed-valence clusters. 2. Iron-sulfur proteins $[Fe_4S_4]^+$ and $[Fe_4S_4]^{3+}$. *J. Struct. Chem.* **1996**, *37*, 699−706.
(54) Belinskii, M. I. Electronic interaction in trimeric mixed valence clusters. *Mol. Phys.* **1987**, *60*, 793−819.
(55) Palii, A.; Clemente-Juan, J. M.; Aldoshin, S.; Korchagin, D.; Golosov, E.; Zilberg, S.; Tsukerblat, B. Can the Double Exchange Cause Antiferromagnetic Spin Alignment? *Magnetochemistry* **2020**, *6*, 36−47.
(56) Tsukerblat, B.; Palii, A.; Clemente-Juan, J. M. Self-trapping of charge polarized states in four-dot molecular quantum cellular automata: bi-electronic tetrameric mixed-valence species. *Pure Appl. Chem.* **2015**, *87*, 271−282.
(57) Tsukerblat, B.; Palii, A.; Clemente-Juan, J. M.; Coronado, E. Mixed-valence molecular four-dot unit for quantum cellular automata: vibronic self-trapping and cell-cell response. *J. Chem. Phys.* **2015**, *143*, 134307−134315.
(58) Kambe, K. J. On the paramagnetic susceptibilities of some polynuclear complex salts. *J. Phys. Soc. Jpn.* **1950**, *5*, 48−51.
(59) Palii, A.; Tsukerblat, B. Tuning of quantum entanglement in molecular quantum cellular automata based on mixed valence tetrameric units. *Dalton Trans.* **2016**, *45*, 16661−16672.
(60) Palii, A.; Zilberg, S.; Rybakov, A.; Tsukerblat, B. Double-dimeric versus tetrameric cells for quantum cellular automata: a semiempirical approach to evaluation of cell−cell responses combined with quantum-chemical modeling of molecular structure. *J. Phys. Chem. C* **2019**, *123*, 22614−22623.
(61) Tsukerblat, B. S. *Group Theory in Chemistry and Spectroscopy*; Dover Publications: Mineola, New York, 2006; pp 1−448.
(62) Tsukerblat, B.; Palii, A.; Clemente-Juan, J. M.; Coronado, E. Modeling the properties of magnetic clusters with complex structures: how symmetry can help us. *Int. Rev. Phys. Chem.* **2020**, *39*, 217−265.
(63) Palii, A.; Tsukerblat, B. Targeting Exchange Interactions in Nanosize Molecular Magnets by Angular Momentum Technique. In *Comprehensive Coordination Chemistry III*; Elsevier, 2020; Chapter 14779.
(64) Zhou, S.; Blair, E. P. Non-Markovian models of environmentally-driven disentanglement in molecular charge qubits. *J. Appl. Phys.* **2020**, *127*, No. 084303.

https://dx.doi.org/10.1021/acs.jpcc.0c08186
J. Phys. Chem. C 2020, 124, 25602−25614

(65) Blair, E. P.; Toth, G.; Lent, C. S. Entanglement loss in molecular quantum-dot qubits due to interaction with the environment. *J. Phys.: Condens. Matter* **2018**, *30*, No. 195602.
(66) Ramsey, J. S.; Blair, E. P. Operator-sum models of quantum decoherence in molecular quantum-dot cellular automata. *J. Appl. Phys.* **2017**, *122*, 084304−084309.
(67) Blair, E. P.; Lent, C. S. Environmental decoherence stabilizes quantum-dot cellular automata. *J. Appl. Phys.* **2013**, *113*, No. 124302.

https://dx.doi.org/10.1021/acs.jpcc.0c08186
J. Phys. Chem. C 2020, 124, 25602−25614